Study of the Granular Electromagnetic Calorimeter with PPDs and Scintillator Strips for ILC

Katsushige Kotera[a], for the CALICE collaboration

[a] *Shinshu University, Matsumoto, Japan*

Abstract

A prototype module of a fine-granular electromagnetic calorimeter has been constructed by the CALICE collaboration and tested in the period Aug. - Sept. 2008 at the FNAL meson beam test facility. The calorimeter is one of the proposed concepts for a highly granular electromagnetic calorimeter for the International Linear Collider (ILC) experiment, which is designed to have an effective 10 mm × 10 mm lateral segmentation using 10 mm × 45 mm scintillator strips. The strips in the 15 odd layers are orthogonal with respect to those in the 15 even layers. A total of 2160 strip scintillators are individually read out using a Pixelated Photon Detector (PPD) or MPPC. As a preliminary result of the first stage analysis, we obtain a relative energy resolution for single electrons of $\sigma_E/E = (15.15 \pm 0.03)\%/\sqrt{E_{\mathrm{beam}}(\mathrm{GeV})} \oplus (1.44 \pm 0.02)\%$, the quoted uncertainties are purely statistical.

Key words: ILC, Electromagnetic calorimeter, Scintillator strip, PPD, MPPC, granular

1. Introduction

The International Linear Collider (ILC) experiments are designed to perform high precision measurements using the clear initial states of the electron-positron collisions and well reconstructed final states. To characterize the final states dominated by gauge bosons and heavy quarks, the reconstruction of jets is one of the key issues. One of the ways to precisely reconstruct jets is to measure individual particles within jets, by combining calorimetry and tracking. This method, called particle flow approach (PFA), requires highly granular calorimeters: finer than 10 mm × 10 mm lateral segmentation for the electromagnetic calorimeter (ECAL) [1].

The Scintillator ECAL (ScECAL) is one of the proposed concepts for a highly granular ECAL for the ILC, which is designed to have an effective 10 mm × 10 mm lateral segmentation using 10 mm × 45 mm scintillator strips. In order to achieve the required 10 mm × 10 mm lateral segmentation, the strips in the odd layers are orthogonal with respect to those in the even layers. The proposed detector is a sampling calorimeter, with sensitive layers made of 2 mm thick plastic scintillator and 3 mm thick absorber layers. The scintillation photons are collected by a wavelength shifting (WLS) fiber, inserted centrally, along the longitudinal direction of each scintillator strip and are read out with a Pixelated Photon Detector (PPD).

A first ScECAL prototype had a transverse area of 90 mm × 90 mm and 26 scintillator layers in between 3.5 mm thick tungsten-cobalt absorber layers [2]. The radiation length of the whole detector was in total 18.5 X_0. This first prototype of the ScECAL was tested using 1 - 6 GeV/c positron beams at DESY in March 2007. The deviation compared with the linear behavior of the energy response was less than 1% indicating the good linearity in this energy range. The stochastic term of the energy resolution curve, 14%, shows a good energy resolution. However, the constant term of the energy resolution curve is found to be 3%. This large constant term is understood because of the shower leakage and the non-uniformities in the response of the strips.

The second prototype was built, transversally twice as large as the first prototype, 180 mm × 180 mm. The number of layers has also been increased to 30 in 266 mm, leading to a total radiation length of 21.3 X_0. Hereafter, the "ScECAL prototype" denotes the second prototype. In the period August - September 2008 and in April - May 2009, the ScECAL prototype was exposed at FNAL to electron and hadronic beams up to 32 GeV/c, together with the analog scintillator hadron calorimeter [3] and the Tail Catcher [4] to evaluate their combined performance in the CALICE test beam activities.

These proceedings explain the analysis to evaluate the linearity and the resolution of the energy measurement by the second ScECAL prototype using electron beam data and muon beam data taken in August - September 2008. The results in these proceedings are very preliminary, because they are estimated without any systematic uncertainty. More detailed analysis results will follow in the near future.

2. Construction of the second ScECAL prototype

The layered structure of the ScECAL prototype is visible in Figure 1, top: it has 30 pairs of scintillator and absorber layers with a thickness of 3.0 mm and of 3.5 mm, respectively. The absorber is made of 88% tungsten, 12% cobalt, and 0.5% carbon. Each scintillator layer (as shown in Figure 1, bottom) has 18 × 4 scintillator strips of the size of 45 mm × 10 mm, made with an extrusion method at Kyungpook National University (KNU). Each scintillator strip is hermetically covered with the reflecting film made by Kimoto Co., Ltd. In successive scintillator

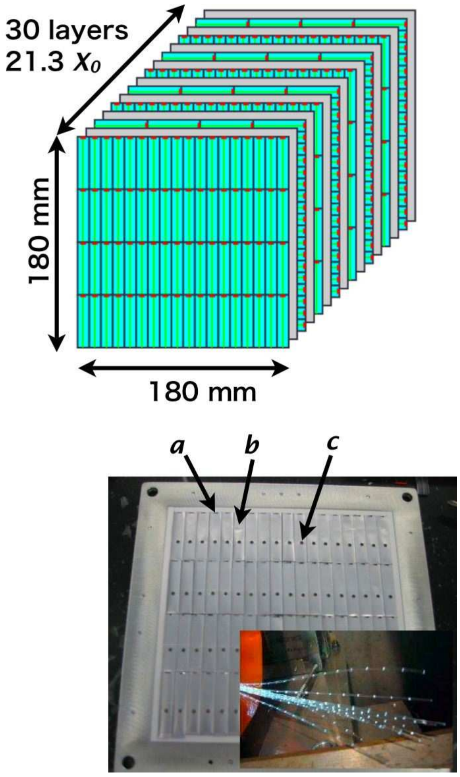

Figure 1: *Top*: structure of the ScECAL prototype in Aug. - Sept. 2008 and Apr. - May 2009 at FNAL. *Bottom*: photo of a sensitive layer showing the PPD housing (*a*), the scintillator strip hermetically covered by a KIMOTO reflector (*b*), and holes to introduce LED light for the gain monitoring system (*c*). The photo in the insert shows the LED light distributed through bundles of clear fibers to each strip through holes in the reflectors (*c*) for calibration purposes.

layers, the strips are alternately aligned vertically ("X" - layers) and horizontally ("Y" - layers). The coordinate system used in these proceedings is right handed and the z direction given by the beam direction. The WLS fibers placed in the center of each strip to collect the scintillation photons are of the Kuraray Co., Ltd. Y-11 double-cladded type. They are read out with PPDs made by Hamamatsu Photonics KK, the "1600-pixel MPPCs". We measured the gain, capacitance, dark noise and breakdown voltage for each MPPC. The MPPCs were then soldered on a flat cable, and mounted in a housing at the end of each scintillator strip. To improve the longitudinal uniformity of the scintillator response, a sheet of reflector film with a hole for the WLS fiber was added between the MPPC package and the scintillator in order to exclude the photons near the sensor but not coming through the WLS fiber.

3. Beams and the experimental setup

The beam test has been performed in the MT6 experimental area at the Meson Test Beam Facility (MTBF) of FNAL. Electron and charged pion beams with a momentum between 1 GeV/c and 32 GeV/c were used. A muon beam at 32 GeV/c was also provided for the calibration with Minimum Ionizing Particles (MIPs).

The electron beam momentum was tuned at 1, 3, 6, 12, 16, 25, and 32 GeV/c.

4. Analysis

4.1. Detector calibration with Minimum Ionizing Particles

The first step in the analysis is the calibration of the strips using muons in order to measure the energy deposition by Minimum Ionizing Particles. This analysis gives the conversion factor between the ADC counts and the number of MIPs. The muon-tuned beam contains almost no electrons nor pions, because of the iron dump put in the beam line upstream of our experiment's site. Therefore, the MIP events are only required to have the same X and Y "hit" positions in at least 10 different X and Y layers, respectively. A "hit" is defined as a signal larger than the mean value of the pedestal by at least three standard deviations of the pedestal.

For each channel, the MIP response is obtained by fitting the distribution of the charge deposited by the MIP events, in ADC counts, with a Landau function convoluted with a Gaussian function. The MIP calibration factor is the most probable value (MPV) of the distribution. The average and the RMS of the MIP calibration factors over the 2160 channels are 160.3 and 31 ADC counts, respectively. The average is significantly larger than the corresponding standard deviation of the pedestal which is 15 ADC counts.

4.2. The correction of the MPPC saturation

The MPPC response has a saturation behavior according to its intrinsic property. Prior to the FNAL beam test, the MPPC saturation was measured on a test-bench. A scintillator strip of the ScECAL prototype was illuminated with a blue laser sending pico-second pulses. The photons which came through one of the two cross sections of the WLS fiber in the strip were read out by a MPPC, and the photons which came through the cross section on the other side were read out by a PMT.

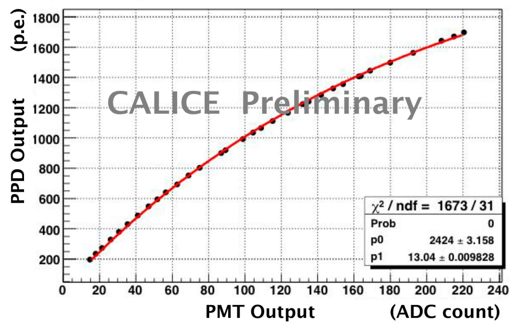

Figure 2: The response of the PPD as a function of the PMT signal in ADC counts. The solid line shows the result of a fit using Eq. (1).

Figure 2 shows the MPPC response as a function of the ADC counts of the photomultiplier. It indicates that the MPPC saturation appears in a region of large light input.

This saturation behavior is represented by:

$$N_{\rm fired} = N_{\rm pix}\left(1 - \exp\left(\frac{-\epsilon N_{\rm in}}{N_{\rm pix}}\right)\right), \quad (1)$$

where $N_{\rm fired}$ is the number of photons detected with the MPPC, $N_{\rm pix}$ is the effective number of pixels on the MPPC, ϵ is the photon detection efficiency, and $N_{\rm in}$ is the number of photons coming into the MPPC sensitive area. By fitting Eq. (1) to the MPPC versus PMT curve in Figure 2, the fitting parameter $N_{\rm pix}$ is determined to be 2424 ± 3. The actual number of pixels is 1600. We think this result shows that the photon generation in the scintillator has a time duration which allows some pixels to be active again in the allocated time window, hence allowing to be hit more than once in an event. In order to apply the correction for each channel, we use the inverse function of the Eq. (1). The input of the function, $N_{\rm fired}$, should be the number of photons detected with the MPPC of the relevant channel. Therefore, the ADC counts of the output signals of the strip should be converted to the number of photons. To convert the ADC counts to the number of photons, the ratio of the ADC counts per photon for each channel has to be known. An LED calibration system [5] to get such ADC-photon ratio was embedded in the ScEAL prototype and the LED calibration data taking were carried out. But, for nearly 30% of all channels, the LED calibration system had problems. Therefore, the average of the ADC-photon ratios of all available channels are used for such channels.

4.3. Energy spectra

Using the set of calibration factors obtained in Section 4.1, the deposited energy is obtained in MIP units by summing the calibrated response over all strips:

$$E_{\rm total} = \sum_{l=1}^{30}\sum_{s=1}^{72} E'_{ls}/c_{ls}, \quad (2)$$

where l and s are the layer and strip indices, E'_{ls} is the measured energy corrected for MPPC saturation, and c_{ls} is the calibration factor for the corresponding strip. The corrected value of the measured energy, E'_{ls}, is obtained as follows:

$$E'_{ls} = -n_{\rm pix}R_{{\rm ADC-photon},ls}\log\left(1-\frac{N_{{\rm ADC},ls}/R_{{\rm ADC-photon},ls}}{n_{\rm pix}}\right), \quad (3)$$

where $n_{\rm pix}$ is the effective number of pixels and $R_{\rm ADC-photon}$ is the ratio of ADC counts to the number of detected photons for each strip (both $n_{\rm pix}$ and $R_{\rm ADC-photon}$ were obtained in the Section 4.2), and $N_{{\rm ADC},ls}$ is the number of ADC counts as the response of each strip.

The spectra of the deposited energy for several beam momenta include some contamination from pions and muons. After implementing certain criteria to purify the electron events, the spectrum of each run is fitted with a Gaussian function.

Figure 3 shows the shape of the spectrum after all cuts for one of the 25 GeV/c runs. The spectrum is fitted well in the range including 90% of the function area, i.e. between ± 1.65 σ. On the other hand, similar distributions for the 1 GeV/c runs show a residual contamination with pions in the lower energy region of the electron peak. We discuss this issue more in Section 5.

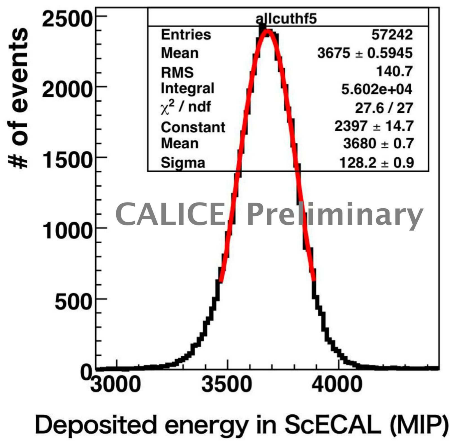

Figure 3: The energy spectrum of a 25 GeV/c run after the complete electron selection, together with a Gaussian fit of the distribution (smooth curve).

The deposited energy and its resolution are determined as the mean value and the standard deviation of the fitted Gaussian function, respectively.

For every selection cut, we investigate the variations of the deposited energy in the ScECAL prototype and its resolution when changing the cut values. It was checked that for any of the applied selection criteria and for all beam momenta, the stability of the deposited energy is better than 0.1% and the resolution stability is better than 1%.

A temperature monitoring was implemented during the data taking, and the overall effect of the temperature variation on each channel was investigated in the May 2009 beam test. As a result, the MIP calibration factors change by 3.5% per one Kelvin. Unfortunately, in September 2008 the temperature monitoring was not very reliable, sometimes leading to noisy or missing data. Although we are still trying to recover the temperature data, the deposited energy and the energy resolution for each beam momentum are calculated as the weighted average of the runs in order to avoid the effect of temperature differences between runs.

5. Results and discussions

5.1. Linearity of the energy response

Figure 4 shows the deposited energy in the ScECAL prototype as a function of the beam momentum. The line indicates the result of a fit with a linear function passing through the origin. Figure 4 shows the good linearity, the deviations from the linear behavior are smaller than 6%.

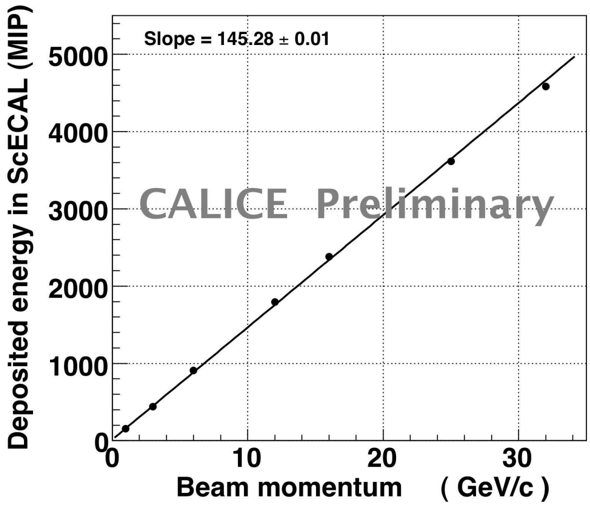

Figure 4: The deposited energy in the ScECAL as a function of the beam momentum. The line shows the results of linear fitting, with forced zero offset.

The MPPC saturation correction is applied according to Eq. (3) which has only one parameter, the number of the effective pixels, $n_{\text{pix}} = 2424$. This number is larger than the actual number of pixels, 1600, because the timing structure of the incoming photons allows some pixels to become active again during the event. Since there is a possibility that the timing structure is depending on the deposited energy and on the incident particle species, the behavior of the MPPC saturation should be studied in more detail and the systematic uncertainty from the MPPC correction should be estimated. Additionally, there is a possibility that a part of the fluctuation of the MIP calibration factors discussed in Section 4.1 comes from the MPPC/Fiber mismatch. In that case, some of the pixels are not covered with WLS fiber, then n_{pix} decreases. The effect of the correction for such a case should increase the size of the MPPC saturation correction. Another possible origin of the deviation is some transverse or longitudinal leakage. We will investigate in detail the MPPC saturation correction and the leakage effects in the near future.

5.2. Resolution of the energy response

Figure 5 shows the resolution of the deposited energy in the ScECAL prototype as a function of the beam momentum. The line is the result of a fit with a quadratic parameterization of the resolution:

$$\frac{\sigma}{E} = \sigma_{\text{constant}} \oplus \sigma_{\text{stochastic}} \frac{1}{\sqrt{E_{\text{beam}}(\text{GeV})}}, \tag{4}$$

where E is the deposited energy in the ScECAL, σ the energy resolution, E_{beam} the beam energy, and σ_{constant} and $\sigma_{\text{stochastic}}$ the constant and the stochastic term of the energy-resolution parameterization, respectively. The stochastic and the constant term of the energy resolution parameterization are 15.15 ± 0.03% and 1.44 ± 0.02%, where the uncertainties are only statistical uncertainties. Compared to the result of the first ScECAL prototype, the constant term of the energy resolution of the second ScECAL prototype is decreased by half. This fact indicates that the uniformity of the response of the strips is drastically improved with respect to the first ScECAL prototype.

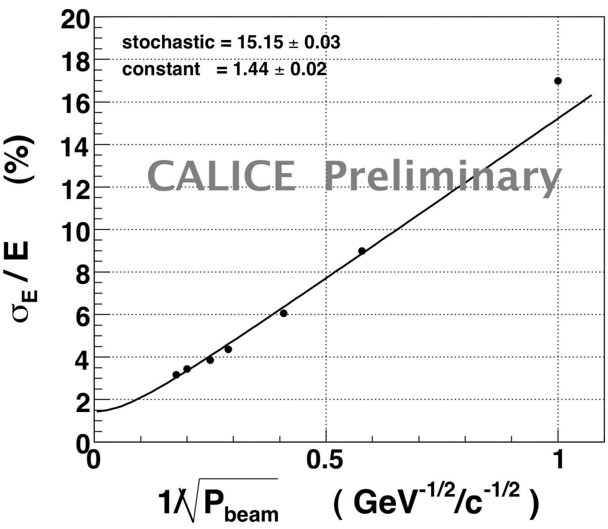

Figure 5: The resolution of the ScECAL energy response as a function of the beam momentum.

The reduced χ^2 of the Gaussian fitting of the energy spectrum is generally around one; with the exception of the 1 GeV/c runs when it is $\sim$ 2.7 because of the tail of the spectrum. The beam used in the FNAL beam test includes both pions and electrons. Although we used the Ĉerenkov counter to select electrons, the electron data have some residual pion contamination. Especially for the 1 GeV/c beam, pion rejection is difficult and after all cuts, the samples still include pions. More effective cuts to reject pions, and the systematic uncertainty from the pion contamination will be studied in the next step.

6. Summary

The ScECAL beam test has been performed using an electron beam in the momentum range of 1 - 32 GeV/c. As a result of this preliminary analysis, the stochastic and constant terms of the energy resolution parameterization are 15.15 ± 0.03% and 1.44 ± 0.02%, where the uncertainties are only statistical uncertainties. The deviations from a linear behavior of the energy measurement are found to be less than 6%. These results are very preliminary because they are estimated without any systematic uncertainties. Further analysis including the temperature correction, the MPPC saturation correction, the energy leakage, and the effect of the pion contamination is ongoing.

References

[1] ILD Concept Group, ”The International Large Detector Letter of Intent” (2009).

[2] CALICE analysis note 012.
“The scintillator ECAL beam test at DESY, June 4, 2008 - Update 3”.

[3] G. Eigen, “The CALICE scintillator HCAL test beam prototype”, AIP Conf. Proc. 867 (2006) 565-573.

[4] A. Dyshkant, “Tail Catcher Muon Tracker for the CALICE test beam”, AIP Conf. Proc. 867 (2006) 592-599.

[5] Ivo Polak, “Development of Calibration system for AHCAL”, ECFA meeting in Valencia (2007).